A Compact Antenna Test Range Based on a Hologram

Taavi Hirvonen, Juha P. S. Ala-Laurinaho, Jussi Tuovinen, *Member, IEEE,* and Antti V. Räisänen, *Fellow, IEEE*

***Abstract*—The application of conventional reflector-type compact antenna test ranges (CATR's) becomes increasingly difficult above 100 GHz. The main problems are the tight surface accuracy requirements for the reflectors and, therefore, the high manufacturing costs. These problems can be overcome by the use of a hologram type of compact range in which a planar hologram structure is used as a collimating element. This idea is described and its performance is studied with theoretical analyses and measurements at 119 GHz.**

***Index Terms*—Antenna measurements.**

I. Introduction

ANTENNA testing of future remote sensing and radio astronomical satellites has given rise to a need for accurate measurements of electrically large reflector antennas at millimeter and submillimeter wavelengths. Previous studies have shown that a compact antenna test range (CATR) has the greatest potential for these kinds of tests [1]. A CATR is commonly realized with the use of one or more reflectors for which the surface accuracy needs to be better than about 0.01 wavelengths. As a result, tight surface-accuracy specifications at frequencies above 100 GHz are required. For example, at 200 GHz the required surface accuracy is 15 μm (rms). The use of a dielectric lens has been studied as a possible alternative to overcome the problems incurred by the use of reflectors with insufficient surface accuracy [2], [3]. Recently, a new concept employing a planar hologram structure as a collimating element to form the desired plane wave in a CATR has been introduced [4], [5]. The hologram CATR is a low-cost easy-to-fabricate structure. The surface-accuracy requirements for an amplitude hologram are less stringent than those for a reflector. On the other hand, a high degree of flatness is easily achieved by stretching the hologram into a frame. As a result, a hologram CATR has great potential for realizing high-quality low-cost compact ranges, even at submillimeter wavelengths.

This paper describes the operational concept of a hologram CATR, briefly reviews the synthesis and features of a computer-generated hologram, and compares theoretical and experimental performance of a hologram CATR at 119 GHz.

Manuscript received October 7, 1996; revised January 30, 1997. This work was supported by the Foundation of Finnish Inventions and the Technology Development Centre.

T. Hirvonen, J. Ala-Laurinaho, and A. Räisänen are with Radio Laboratory, Helsinki University of Technology, Helsinki, FIN-02015 HUT Finland.

J. Tuovinen is with the Millimeter Wave Laboratory of Finland, MilliLab, Espoo, FIN-02150 Finland.

Publisher Item Identifier S 0018-926X(97)05597-X.

This work is a part of an international project to develop the Odin satellite, which will carry a millimeter- and submillimeter-wave radio telescope. The radio telescope uses an offset reflector antenna and a main reflector with diameter 1.1 m designed to operate with heterodyne receivers at frequency bands 119, 486–504, 541–558, 547–564, and 563–580 GHz. The antenna will be tested with a hologram CATR at 119 GHz.

II. Hologram CATR

Microwave holography has many applications. Some involve long distance; others involve small scale. The applications of microwave holography are reviewed in [6]. Microwave holograms can be used as antennas. The hologram antenna is illuminated with microwaves and the hologram diffracts to form the desired far-field pattern. However, holograms have not previously been used in CATR's to produce a desired Fresnel region field (radiating near field). We have shown by theoretical analyses and measurements that holograms are applicaple for CATR's as well.

Fig. 1 illustrates a facility layout employing a hologram CATR. The feed horn transmits a spherical wave onto one side of a computer-generated amplitude hologram structure that modulates the field such that a planar wave is emanated on the other side of the structure. The antenna under test (AUT) is illuminated with this plane wave. The extent of the volume enclosing the plane wave is called the quiet-zone. The required field-quality of the quiet-zone is driven by the required measurement accuracy of the AUT. Typical requirements are a peak-to-peak amplitude ripple less than 1 dB and phase ripple less than 10° in the quiet-zone [1]. The hologram is placed in an opening in the wall that divides the anechoic chamber into two parts. This dividing wall also shields the AUT from direct-feed radiation.

In general, a hologram structure changes both the amplitude and phase of a field transmitted through or reflected from the structure. In practice, holograms are usually realized so that they modulate only the amplitude or the phase of the field. The resulting hologram is correspondingly referred to as either an amplitude or a phase hologram. The latter alternative is also sometimes called a kinoform [7]. A transmitting amplitude hologram, like the one used here for the compact range, can be approximated by an appropriately shaped pattern etched to a thin metal layer on a dielectric film (substrate).

The manufacturing process of an amplitude hologram is relatively inexpensive—only a few percent of the cost of a comparably sized curved reflector. The hologram can be

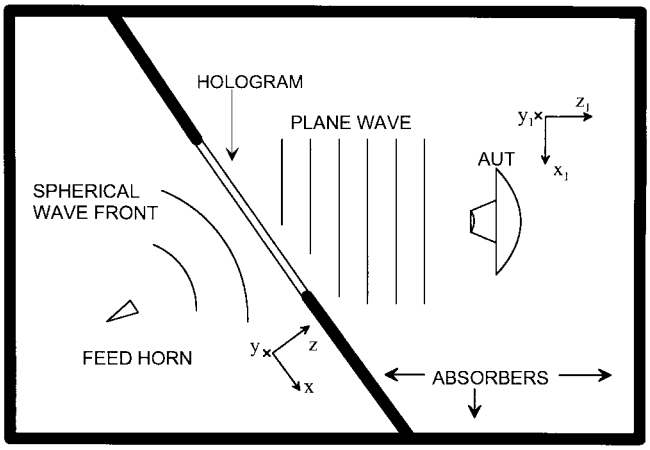

Fig. 1. Measurement arrangement for a hologram CATR.

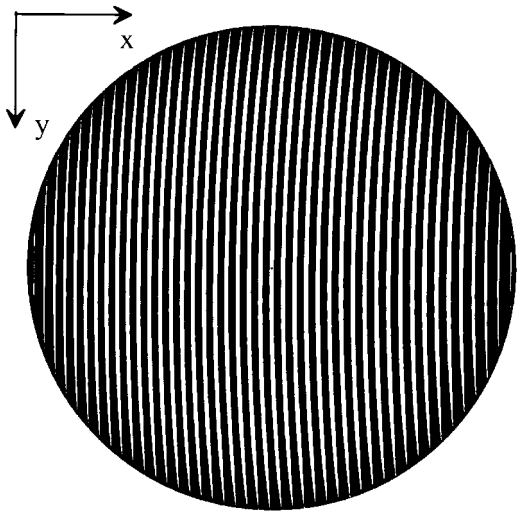

Fig. 2. An example of a binary amplitude hologram pattern. Nontransparent and transparent parts are shown with black and white, respectively.

manufactured with an etching process similar to that used for making printed circuits. Since the hologram is a transmission-type device, the surface accuracy requirement is less stringent than that of a reflector. Furthermore, a highly planar surface is easy to achieve for the hologram since it is streched into a frame [8]. The disadvantages of a hologram are the fairly strong dependence on frequency and polarization. The frequency dependence of a hologram has been discussed in [4] and [9].

III. Generation of a Hologram

Generating a conventional hologram means creating an interference pattern of two wavefronts on a surface. After the hologram has been created, one of the interfering fields can be recreated by illuminating the hologram with the other interfering field. A hologram can be simply formed at optical wavelengths by illuminating a photosensitive film with two light beams, (a light reflected from an object and a reference light).

In many practical applications, in the optical and radiowave region, holograms, i.e., interference patterns are synthesized by computational methods [computer-generated hologram (CGH)]. The hologram pattern is determined by numerically calculating the structure required to change the known input field into the desired output field. Due to fabrication limitations, the structure of the hologram has to be quantized in some way. The method for accomplishing this is usually called the coding scheme of the CGH. The two most widely used schemes are the binary phase and binary amplitude quantizations in which either the phase or amplitude transmittance of the hologram is limited to two different discrete values [7]. For example, the binary amplitude hologram either lets the incoming light pass through undisturbed (transmittance $= 1$) or blocks it completely (transmittance $= 0$).

The transmittance $T(x', y')$ of a general amplitude hologram can be written as [10], [11]

$$T(x', y') = \frac{1}{2}\{1 + a(x', y')\cos[\Psi(x', y')]\} \tag{1}$$

where x', y' are the coordinates in the hologram plane and $a(x', y')$ is a real function proportional to the relation between the output and input amplitudes so that the hologram compensates the amplitude variation of the input field and adds an amplitude taper to the amplitude of the output field. The phase term is $\Psi(x', y') = \psi(x', y') + 2\pi\nu x'$ where ν denotes the spatial carrier frequency, which separates the diffraction orders produced by the hologram. The desired output field leaves the hologram at an angle of

$$\theta = \arcsin(\nu\lambda) \tag{2}$$

so that the unwanted diffraction orders do not disturb the quiet-zone field. The normalized phase of the input field (feed horn) in the plane of the hologram is $\psi(x', y')$.

The transmittance of the corresponding binary-amplitude coded hologram is given by (see also [7], [10])

$$T_B(x', y') = \begin{cases} 0, & 0 \le \frac{1}{2}[1 + \cos\Psi(x', y')] \le b \\ 1, & b < \frac{1}{2}[1 + \cos\Psi(x', y')] \le 1 \end{cases} \tag{3}$$

where

$$b = 1 - (1/\pi)\arcsin a(x', y').$$

The phase is modulated by the locations of the slots and the amplitude is modulated by the variations of the slot widths. The main effect of the binarization is the redistribution of energy between the various diffraction orders of the hologram.

Fig. 2 shows an example of a binary amplitude hologram pattern used in the measurements described later. This pattern is derived from a known incident field, i.e., feed-horn spherical wave and a required aperture field, which radiates a plane wave to the quiet zone. The plane wave is designed to leave the hologram in an angle of 33.0°. If no taper is used, the slot edges are arcs of circles with a common center. The distances between slots and the slot widths increase toward the common center.

IV. Theoretical Analysis of a Hologram CATR

The field in the quiet zone is calculated by using an exact near-field aperture integration [physical optics (PO)] together

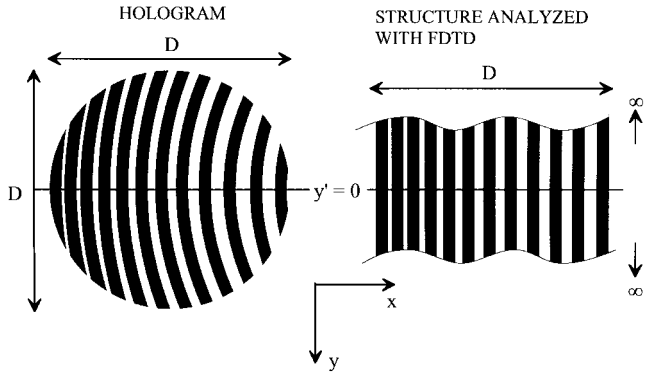

Fig. 3. The structure of the hologram and the structure, which is used in the theoretical analysis.

with a finite-difference time-domain (FDTD) analysis. The formula for the quiet-zone field is

$$\mathbf{E}(x,y,z) = \int_S E_a(x',y')\frac{1+jkR}{2\pi R^3}e^{-jkR} \times [\mathbf{u}_y(z-z') - \mathbf{u}_z(y-y')]\,dS' \qquad (4)$$

where $R = \sqrt{(x-x')^2+(y-y')^2+(z-z')^2}$ is the distance from a point in the aperture (hologram) to a point in the quiet zone. In (4), the polarization of the feed antenna is assumed to be in the $\mathbf{u}_y$ direction. For the case of $\mathbf{u}_x$ polarization we must have $\mathbf{u}_x(z-z') - \mathbf{u}_z(x-x')$ in the brackets [3].

The transmittance function $T_B(x',y')$ (3) determines the binary structure of the hologram (i.e., the areas where the metal is etched off). In practice, however, the function is insufficient to describe the actual transmission through the narrow slots of the hologram because the transmission depends on the polarization and the width of the slot. $E_a(x',y')$ in (4) is the complex field in the aperture of the hologram, which is calculated with a two-dimensional (2-D) (xz plane) FDTD analysis. The FDTD prediction was performed across the hologram at a fixed value of y' using the complex field of the feed horn ($\mathbf{E}_{\text{feed}}(x',y')$) in the plane of the hologram as an excitation. In this case, $\mathbf{E}_{\text{feed}}(x',y')$ is the radiation pattern of a corrugated horn. The area over which the FDTD analysis is performed in the xz plane is 570 × 3 mm^2 (the diameter of the hologram is 550 mm). In the y dimension, the structure is assumed to be infinite (Fig. 3). Fig. 4 shows the predicted amplitude and phase of $E_a(x',y')$ in the centermost slot of the hologram for vertical and horizontal polarizations. The slight asymmetry of the fields is a result of an offset of the slot location from the exact center of the hologram. The FDTD analysis is more thoroughly explained in [12].

Applying the FDTD analysis incrementally across the entire hologram ($-D/2 \le y' \le D/2$) produces the near-field result which can be integrated (PO) over the hologram surface to produce the quiet-zone field. Analyzing a single hologram in this way would be prohibitively time consuming, taking several months of CPU time on a super computer. However, because the hologram varies slowly with respect to the y' coordinate, it is sufficient to perform the FDTD analysis at a given $y' = y_n$ and calculate the PO integration over one line

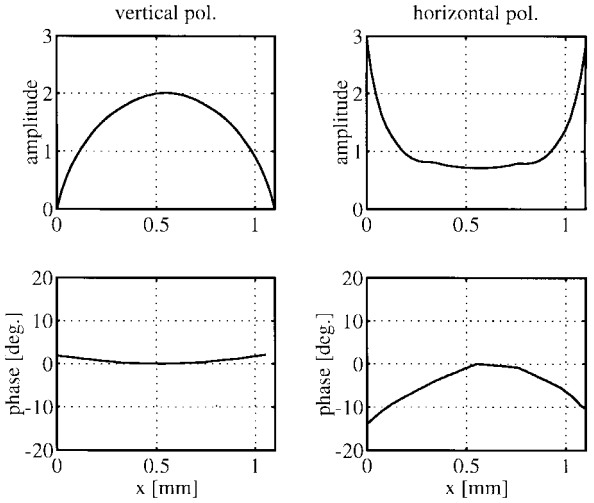

Fig. 4. Aperture electric field in a slot with a vertical and a horizontal polarization.

in the x direction from $-D/2$ to $D/2$, and evaluate the quiet-zone field in the xz plane at the corresponding $y = y_n$. This is validated by comparison of theoretical and experimental results.

To produce a flat amplitude and phase distribution in the quiet zone, the amplitude of the aperture field $|E_a(x',y')|$ is modified with an appropriate weighting function $W(\rho')$ in the term $a(x',y')$ (3). The analysis was performed at $y' = 0$ and the following function was used:

$$a(x',y') = \frac{W(\rho')}{|E_{\text{feed}}(x',y')|} = \frac{0.75\cos^{10}[(2\rho'/D)^2][1.7-0.9\cos(2\rho'/D)]w(x')}{|E_{\text{feed}}(x',y')|} \qquad (5)$$

where

$\rho' = \sqrt{x'^2+y'^2}$

$D =$ diameter of the hologram, 0.55 m

$$w(x') = \begin{cases} 0.94 - 0.06\cos(10\pi(x'-0.07)), & x'[\text{m}] \in [-0.03, 0.17] \\ 1.0, & \text{elsewhere.} \end{cases}$$

The first part of the weighting function ($\cos^{10}[(2\rho'/D)^2]$) tapers the amplitude toward the edge of the aperture to minimize the edge diffraction. The second (symmetric) and third (asymmetric) parts [$[1.7-0.9\cos(2\rho'/D)]$ and $w(x')$] are necessary to appropriately shape the aperture field. The constant 0.75 scales the widths of the slots. $a(x',y')$ determines the widths of the slots and, finally, the 2-D FDTD analysis gives the actual aperture field $E_a(x',y')$ to be integrated.

The phase in the quiet zone can be tuned by adding an extra term to the phase term $\Psi(x',y') = \psi(x',y') + 2\pi\nu x' + \psi_e(x')$ where $\psi_e(x') \ll 2\pi\nu x'$. $\Psi(x',y')$ determines the locations of the slots and even small changes in this term have a significant effect on the phase in the quiet zone, but very little effect on the amplitude. In the case of this experimental hologram, an extra term in phase was not used. In a case of a large hologram, the analysis must be made with several values of y'

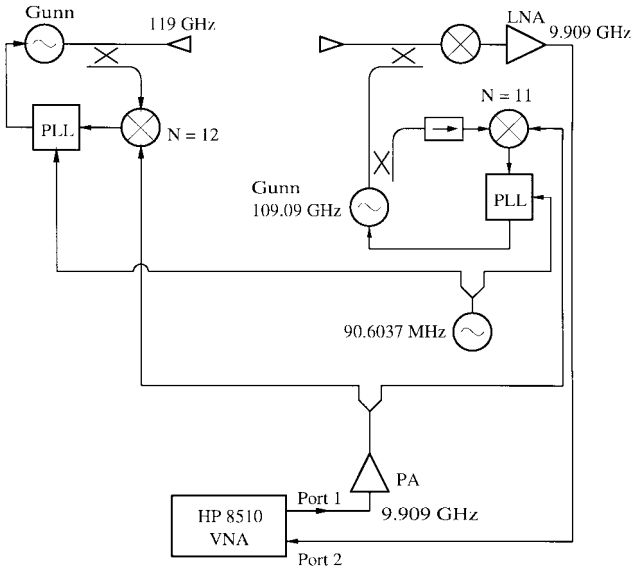

Fig. 5. Measurement setup.

and the weighting function becomes more complicated. Also, the phase has to be tuned by adding an appropriate extra phase term.

Designing a hologram for a near-field application is an iterative procedure, which can be summarized as follows.

1) A weighting function $W(\rho')$ is selected. Function $a(x', y')$ determines the widths of the slots.
2) The hologram is generated by using (3).
3) The quiet-zone field (amplitude and phase) is calculated by using (4). If the result does not meet the requirements, return to step 1) and modify the weighting function $W(\rho')$.
4) If the phase is not flat enough, it can be tuned by adding an extra term to $\Psi(x', y')$. After this change, go back to step 2), and continue until a satisfactory result is achieved.

V. Experimental Analysis of a Hologram CATR

To verify the usefulness of a hologram CATR, an experimental setup was constructed and measurements were carried out at 119 GHz. A 550-mm diameter circular hologram was fabricated on a copper-plated Kapton film using a standard etching procedure. The corrugated horn used as the feed was placed approximately 1.7 m away from the hologram and provided a 3-dB edge taper on the input side of the hologram. The structure of the hologram optimized the quiet-zone field at vertical polarization.

Fig. 5 shows the setup used for measuring the quiet-zone amplitude and phase at 119 GHz. The probe antenna is moved in the quiet-zone using a 1.5 × 1.5 m^2 planar scanner from Orbit Advanced Technology Co. The planarity of the scanner has been measured to be better than 20-μm rms.

In Fig. 1, the center of the quiet zone is at $x_1 = y_1 = 0$. The quiet-zone field was theoretically analyzed in the x_1 direction at two linear polarizations. The measurements were carried out at these polarizations over the whole quiet-zone area.

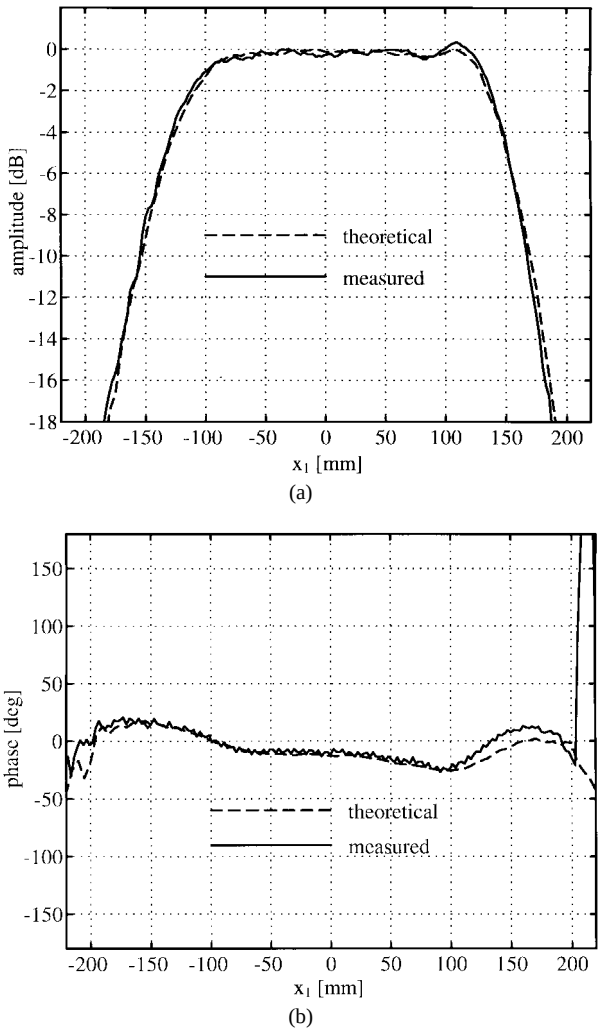

Fig. 6. Theoretical and measured quiet-zone field with a vertical polarization at 119 GHz in the x_1 direction $(y_1 = 0)$. The diameter of the hologram is 550 mm.

Fig. 6 shows the theoretical and measured fields for vertical polarization at 119 GHz in the x_1 direction $(y_1 = 0)$ 1.5 m behind the hologram at an angle 33.0° off the normal of the hologram. The agreement between the theoretical and measured results is excellent—the theoretical amplitude ripple is 0.4 dB (peak-to-peak) and the measured ripple is 0.8 dB occurring mainly at the right end of the quiet zone. The theoretical phase ripple is less than 5°, and the measured ripple is less than 10°, excluding the slight phase tilt. The phase tilt is caused by the complex transmission coefficient of the slots (Fig. 4), i.e., the phase is also slightly changed in the transmission, meaning that instead of 33.0° with respect to the normal of the hologram, the plane wave leaves the hologram in an angle of 32.96°. However, the shape of the quiet-zone phase was not optimized. In an optimized case, the flat-phase area would be somewhat larger and the phase ripple would be smaller. Fig. 7 shows measured result in the y_1 direction $(x_1 = 0)$ where the peak-to-peak ripples are 0.5 dB and 10°. The measured result in the y_1 direction is very good even though the hologram was designed based on the theoretical analysis in a single x cut $(y' = 0)$ only. Fig. 8 shows the 2-D distribution of the quiet-zone field amplitude

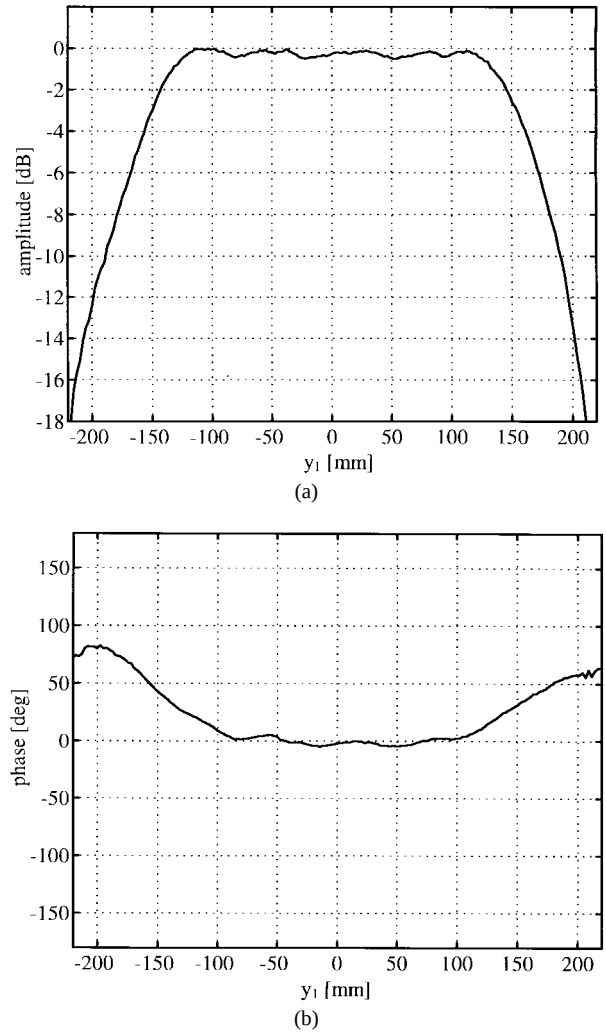

Fig. 7. Measured quiet-zone field in the y_1 direction $(x_1 = 0)$ with vertical polarization at 119 GHz.

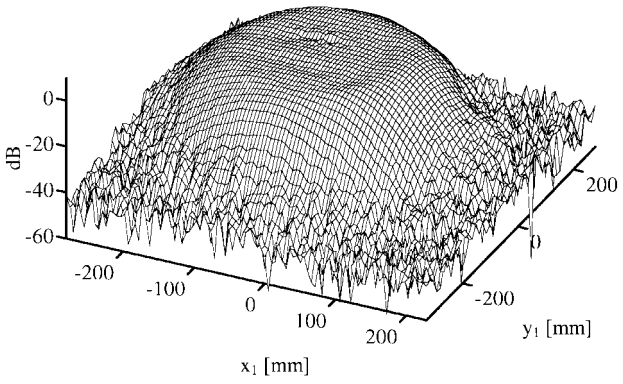

Fig. 8. A three-dimensional (3-D) measurement result of the quiet-zone field amplitude with vertical polarization at 119 GHz.

1.5 m behind the hologram. Fig. 9 shows the theoretical quiet-zone field amplitude in the x_1 direction $(y_1 = 0)$ from 0.8 to 2.5 m behind the hologram; the region at the left of the plot ($x_1 < -200$ mm, $z_1 < 1200$ mm) corresponds to undiffracted fields normal to the hologram. The quality of the quiet zone at vertical polarization is very good; additional iterations in the design procedure could improve the results further.

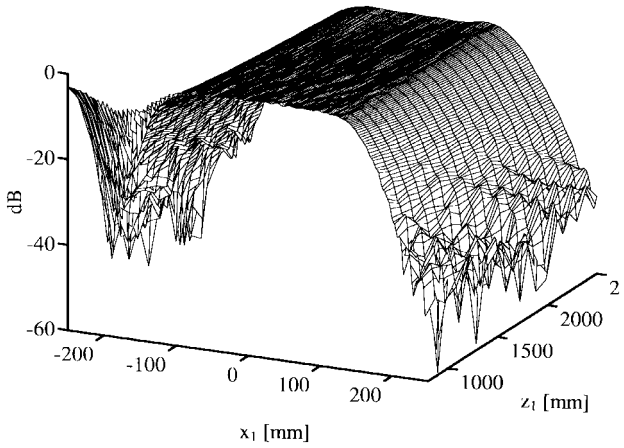

Fig. 9. Theoretical quiet-zone field amplitude in the $x_1 z_1$ plane $(y_1 = 0)$ 0.8–2.5 m behind the hologram.

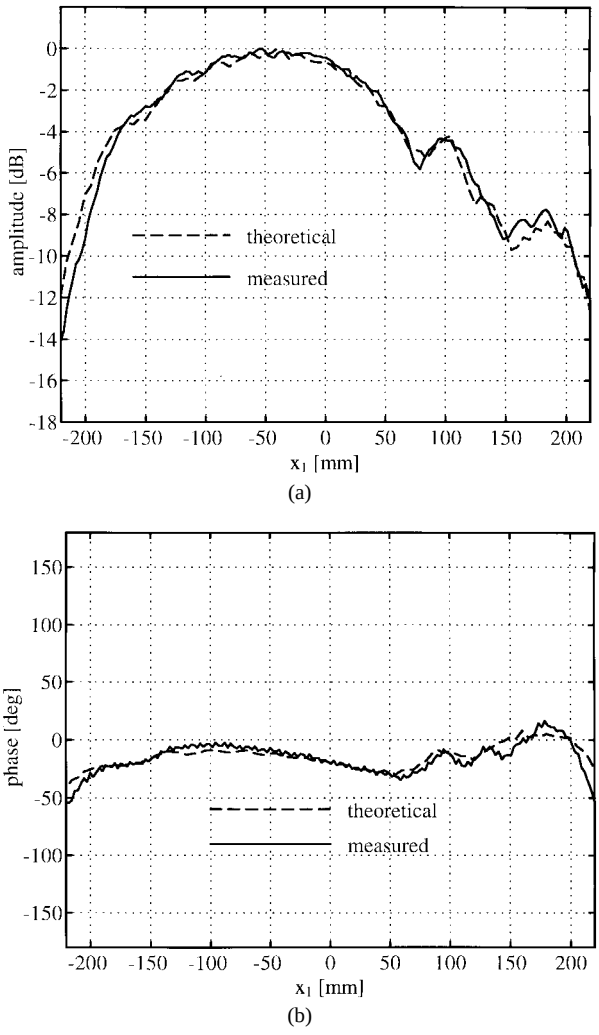

Fig. 10. Theoretical and measured quiet-zone field with horizontal polarization at 119 GHz in the x_1 direction $(y = 0)$.

Figs. 10 and 11 show theoretical and measured results for horizontal polarization in the x_1 direction and in the y_1 direction, respectively. Again, the agreement between theoretical and measured results is excellent. The dense phase ripple (Figs. 6 and 10) is caused by the vibration of the scanner

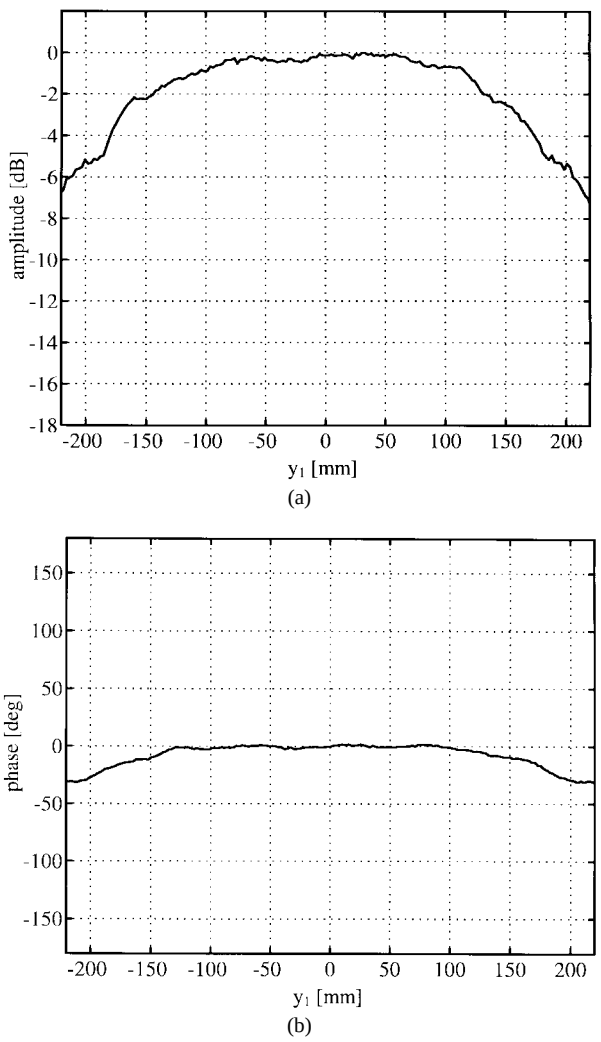

Fig. 11. Measured quiet-zone field in y_1 direction $(x_1 = 0)$ with horizontal polarization at 119 GHz.

when scanned in the horizontal direction (x_1 direction). When scanned in the vertical direction, the scanner was more stable, and the measured phase is smooth. These results show the strong polarization dependence of the hologram, due to an amplitude taper of the hologram, which is realized by making the slots of the hologram narrower toward the edge (5). To reduce the polarization sensitivity, it may be possible to use a set of small collimating reflectors in front of the hologram feed. A potential advantage of this approach is that the amplitude taper of the aperture field would be created by the feed system rather than by the slots of the hologram. This possibility will be studied further in the future.

Because the locations of the slots is determined by the phase of the incoming field, a hologram is a frequency dependent component. The useful bandwidth of a hologram CATR is case specific, i.e., it depends on the size of the hologram compared to the wavelength, the focal length of the hologram, the aperture weighting function (5), and the feed antenna. In this case, the frequency dependence was studied with theoretical and experimental analysis. The most distinct effect of a frequency change is the change in the direction of the plane wave (2), which changes the size of the quiet zone. Other effects are the increased amplitude and phase ripple in the quiet zone and the phase distribution in the quiet zone becoming curved instead of being flat. These effects are due to changes in the radiation pattern of the corrugated horn-feed antenna and in the transmission coefficients of the slots due to the changed wavelength. The phase curvature can be compensated with an axial feed movement, while the quiet-zone amplitude and phase ripple remain almost unchanged. Ultimately, the useful bandwidth depends on the requirements of the quiet-zone amplitude and phase ripple. For example, if a 1-dB peak-to-peak theoretical amplitude ripple is allowed (instead of the 0.4 dB in the "ideal" case), the useful bandwidth is about $\pm 10\%$.

The quiet-zone is 200×240 mm^2 (43% of the diameter of the hologram) and the projection of the hologram (for an angle of 33°) is 460×550 mm^2. The relatively small size of the quiet zone is a consequence of the amplitude taper in the aperture, which must extend over a certain number of wavelengths; in this case about 70λ. An elliptic hologram for Odin telescope tests at 119 GHz (2.4×2.0 m^2) has been analyzed theoretically, the diameter of the quiet zone is about 1.4 m (70% of the diameter of the hologram), and the length of the amplitude taper is about 110λ. A larger hologram is capable of yielding a greater percentage of the physical area for the quiet zone than a smaller hologram. The hologram for Odin telescope testing is under fabrication at the time of this report.

VI. Conclusion

A hologram type of CATR has been described. This novel method utilizes a computer-generated amplitude hologram to form the desired plane wave from the feed horn spherical wave. A hologram CATR is a low-cost alternative for the conventional reflector compact range. Due to the less stringent surface-accuracy requirements, a hologram CATR constitutes an effective method for measuring electrically large millimeter- and submillimeter-wave antennas. The usefulness of this new method was shown by careful theoretical analyses and measurements at 119 GHz for a hologram of a diameter of 550 mm.

Acknowledgment

The authors would like to thank the reviewers for helping us in the style and grammar of this paper.

References

[1] J. Aurinsalo, S. Karhu, A. Koivumäki, R. Pitkäaho, A. Lehto, A. Räisänen, T. Tolmunen, and J. Tuovinen, "Test methods and ranges for testing the millimeter wave sounder of the Meteosat second generation satellites," Final Rep., ESTEC Contract 7966/88/NL/PB(SC), Mar. 1990.

[2] A. D. Olver and A. A. Saleeb, "Lens-type compact antenna test range," *Electron. Lett.*, vol. 15, no. 14, pp. 409–410, 1979.

[3] T. Hirvonen, J. Tuovinen, and A. Räisänen, "Lens-type compact antenna test range at mm-waves," in *Proc. 21st Eur. Microwave Conf.*, Stuttgart, Germany, Sept. 1991, pp. 1079–1083.

[4] J. Tuovinen, A. Vasara, and A. Räisänen, "A new type of compact antenna test range," in *Proc. 22nd Eur. Microwave Conf.*, Espoo, Finland, Aug. 1992, pp. 503–508.

[5] ——, "Compact antenna test range," Finland patent 88750, 1993.

[6] G. Tricoles and N. H. Farhat, "Microwave holography: Applications and techniques," *Proc. IEEE*, vol. 65, pp. 108–121, Jan. 1977.
[7] W.-H. Lee, "Computer-generated holograms: Techniques and applications," in *Progress in Optics XVI*, E. Wolf, Ed. Amsterdam, The Netherlands: North-Holland, pp. 121–231, 1978.
[8] P. R. Foster, D. Martin, C. Parini, A. Räisänen, J. Ala-Laurinaho, T. Hirvonen, A. Lehto, T. Sehm, J. Tuovinen, F. Jensen, and K. Pontoppidan, "Mm wave antenna testing techniques—Phase 2," MAAS Rep. 304, ESTEC Contract 11641/95/NL/PB(SC), 1996.
[9] T. Hirvonen, J. Tuovinen, and A. Räisänen, "Tolerance analysis of a 500 GHz amplitude hologram," in *Proc. 6th Int. Symp. Space Terahertz Technol.*, Pasadena, CA, Mar. 1995, pp. 397–406.
[10] A. Vasara, J. Turunen, and A. T. Friberg, "Realization of general nondiffracting beams with computer-generated holograms," *J. Opt. Soc. Amer.*, vol. 6, pt. A, pp. 1748–1754, 1989.
[11] J. J. Burch, "A computer algorithm for the synthesis of spatial frequency filters," *Proc. IEEE*, vol. 55, no. 4, pp. 599–601, Apr. 1967.
[12] J. Ala-Laurinaho, T. Hirvonen, J. Tuovinen, and A. V. Räisänen, "Numerical modeling of a nonuniform grating with FDTD," *Microwave Opt. Technol. Lett.*, to be published.

Taavi Hirvonen was born in Kannonkoski, Finland, on October 23, 1966. He received the Dipl.Eng. (M.Sc.) and the Lic.Technol. degrees in electrical engineering from the Helsinki University of Technology, Espoo, Finland, in 1991 and 1993, respectively. He is currently working toward the Doctor of Technology degree at the same university.

Since 1991, he has been a Research Engineer at the Radio Laboratory of the Helsinki University of Technology, Espoo, Finland. His current research interest is the development of the quasi-optical methods for antenna measurements.

Juha P. S. Ala-Laurinaho was born in Parkano, Finland, on July 4, 1969. He received the Dipl.Eng. (M.Sc.) degree from the Department of Mathematics and Systems Analysis, Helsinki University of Technology, Espoo, Finland, in 1995. He is currently working toward the Doctor of Technology degree at the same university.

Since 1996, he has been a Research Engineer at the Radio Laboratory of the Helsinki University of Technology, Espoo, Finland. His current research interest is the implementation of finite-difference time-domain (FDTD) in practical electromagnetic problems.

Jussi Tuovinen (S'86–M'91) received the Dipl.Eng., Lic.Technol., and Dr.Technol. degrees in electrical engineering from the Helsinki University of Technology (HUT), Espoo, Finland, in 1986, 1989, and 1991, respectively.

From 1986 to 1991, he worked as a Research Engineer at HUT Radio Laboratory, Espoo, Finland, where he was involved with millimeter-wave antenna testing for the European Space Agency, quasi-optical measurements, and Gaussian beam theory. From 1991 to 1994 he was with the Five College Radio Astronomy Observatory as a Senior Postdoctoral Research Associate, at the University of Massachusetts, Amherst, where he studied holographic testing methods and developed frequency multipliers up to 1 THz. From 1994 to 1995 he was a Project Manager at HUT Radio Laboratory, involved with hologram compact antenna test range (CATR) and 119-GHz receiver development for Odin satellite. Since 1996 he has been a Docent at HUT. Currently he is Director of the Millimeter Wave Laboratory of Finland–MilliLab, ESA External Laboratory, Espoo, Finland.

Dr. Tuovinen received a European Space Agency Fellowship for the multiplier work at the University of Massachusetts, Amherst, in 1992 and 1993. He was a secretary of the Finnish National Committee of COSPAR (Committee on Space Research) and the IEEE Finland Section. He was also the Executive Secretary of the Local Organizing Committee of the 27th Plenary Meeting of COSPAR held in 1988. He is currently a Vice-Chairman of the IEEE MTT/AP Finland Chapter.

Antti V. Räisänen (S'76–M'81–SM'85–F'94) was born in Pielavesi, Finland, on September 3, 1950. He received the Diploma Engineer (M.Sc.), the Licentiate of Technology, and the Doctor of Technology degrees in electrical engineering from Helsinki University of Technology (HUT), Espoo, Finland, in 1973, 1976, and 1981, respectively.

From 1973 to 1978, he was a Research Assistant at HUT Radio Laboratory. From 1978 to 1979, he was a Research Assistant at Five College Radio Astronomy Observatory (FCRAO) of the University of Massachusetts, Amherst. From 1980 to 1983, he was a Research Fellow of the Academy of Finland, working mainly at HUT, but also for shorter periods at FCRAO and Chalmers University of Technology, Gothenburg, Sweden. In 1984, he was a Visiting Scientist at the Department of Physics, University of California, Berkeley. From 1985 to 1989, he was an acting Professor of Radio Engineering with HUT, working also for short periods at the University of California, Berkeley. In 1989, he was appointed by invitation to the Professor Chair of Radio Engineering with HUT. In 1992 and 1993 he was on sabbatical from HUT and had a Senior Research Fellowship from the National Research Council at the Jet Propulsion Laboratory, Pasadena, CA. He was also a Visiting Associate in Electrical Engineering at the California Institute of Technology, Pasadena. Currently, he is supervising research in millimeter components, antennas and receivers, microwave propagation in satellite links, microwave measurements, ect. at HUT Radio Laboratory. He has authored and co-authored more than 250 scientific or technical papers and four books: *Microwave Measurement Techniques*, *Radio Engineering*, *RF and Microwave Techniques*, and *Millimeter Wave Techniques* (Finland: Otatieto, 1991, 1992, 1994, and 1997, respectively, all in Finnish).

Dr. Räisänen was the Secretary General of the 12th European Microwave Conference (1982). He was the Counselor of the IEEE Student Branch in Helsinki from 1982 to 1989 and the Chairman of the IEEE MTT/AP Chapter in Finland from 1987 to 1992. In 1992, he served as the Conference Chairman for the 22nd European Microwave Conference. Currently, he serves in the Research Council for Nature Sciences and Engineering, the Academy of Finland. In 1997, he was elected the Vice-Rector of Helsinki University of Technology for the period of 1997–2000.